Isomeric levels in ^{92}Rb and the structure of neutron-rich ^{92,94}Rb isotopes

W. Urban, K. Sieja, G. S. Simpson, T. Soldner, T. Rząca-Urban, A. Złomaniec, I. Tsekhanovich, J. A. Dare, A. G. Smith, J. L. Durell, J. F. Smith, R. Orlandi, A. Scherillo, I. Ahmad, J. P. Greene, J. Jolie, and A. Linneman

Phys. Rev. C **85**, 014329 — Published 30 January 2012

DOI: 10.1103/PhysRevC.85.014329

Isomeric levels in ^{92}Rb and the structure of neutron-rich ^{92,94}Rb isotopes.

W. Urban,[1,2] K. Sieja,[3,4] G. S. Simpson,[5] T. Soldner,[1] T. Rząca-Urban,[2]
A. Złomaniec,[2] I. Tsekhanovich,[6] J. A. Dare,[7] A.G. Smith,[7] J.L. Durell,[7] J. F. Smith,[7]
R. Orlandi,[7] A. Scherillo,[8] I. Ahmad,[9] J. P. Greene,[9] J. Jolie,[10] and A. Linneman[10]

[1]*Institut Laue-Langevin, 6 rue J. Horowitz, 38042 Grenoble, France*
[2]*Faculty of Physics, University of Warsaw, ul. Hoża 69, 00-681 Warsaw, Poland*
[3]*Université de Strasbourg, IPHC, 23 rue du Loess, 67037 Strasbourg, France*
[4]*CNRS, UMR7178, 67037 Strasbourg, France*
[5]*LPSC, Université Joseph Fourier Grenoble 1, CNRS/IN2P3,*
Institut National Polytechnique de Grenoble, F-38026 Grenoble Cedex, France
[6]*Université de Bordeaux-1/CENBG, 33175 Gradignan Cedex, France*
[7]*Department of Physics and Astronomy, The University of Manchester, M13 9PL Manchester, UK*
[8]*Rutherford Appleton Laboratory, Chilton, Didcot OX11 0QX, United Kingdom*
[9]*Argonne National Laboratory, Argonne, Illinois 60439, USA*
[10]*Institut für Kernphysik, Universität zu Köln, Zülpicherstr. 77, 50937 Köln, Germany*

The medium-spin structure of the ^{92}Rb nucleus, populated in spontaneous fission of ^{248}Cm and ^{252}Cf has been studied using the EUROGAM2 and the GAMMASPHERE Ge arrays, respectively. Two isomers have been found in ^{92}Rb at 284.2 keV and 1958.2 keV with halflives of $T_{1/2}$= 54(3) ns and $T_{1/2}$ = 7(2) ns, respectively. A measurement of neutron-induced fission of ^{235}U, at the PF1B cold-neutron beam facility of ILL Grenoble has been performed to confirm the assignment of the $T_{1/2}$= 54(3) ns, 284.2-keV isomeric level to the ^{92}Rb nucleus. Excited levels in ^{92}Rb and ^{94}Rb nuclei have been calculated in a large-scale shell-model framework. Isomers observed in these two nuclei have been interpreted as proton-neutron configurations involving the high-j $\nu 1h_{11/2}$ and $\pi 1g_{9/2}$ orbitals.

PACS numbers: 21.10.Tg, 23.20.Lv, 25.85.Ec, 27.60.+j

I. INTRODUCTION

This work is part of a program to measure and to understand the structure of neutron-rich, spherical nuclei located on the nuclear chart "north-east" of the ^{78}Ni nucleus, expected to be a doubly-closed-shell core for this region. Some of these nuclei, being accessible experimentally, are expected to lie on the path of the astrophysical r-process. Therefore, they could provide data for modeling this important nucleosynthesis process, an opportunity available for a limited number of nuclei, only.

The low-neutron and low-proton limits of the discussed region of neutron-rich, spherical nuclei are defined by the N=50 and Z=28 shell closures (though it is not known if the Z=28 shell closure will continue for N>50), while upper borders are set at N=58 and Z=40. At N=56 there is a distinct subshell gap, corresponding to the closure of the $\nu 2d_{5/2}$ shell, but spherical shapes are observed up to N=58, due to the filling of the $\nu 3s_{1/2}$ orbital present nearby. Analogously, on the proton side, there is a subshell closure at Z=38 due to closing of the $\nu 2p_{3/2}$ and $\nu 1f_{5/2}$ subshells, followed by a subshell closure at Z=40 due to the $\nu 2p_{1/2}$ spherical subshell.

Because of the Z=38 subshell closure, the $^{88}Sr_{50}$ semi-magic nucleus has been often used as a core for shell-model calculations in this region, though not always successfully [1]. The doubly-closed-shell nucleus ^{78}Ni should be a better core for calculations at $Z \approx$38, and indispensable when describing nuclei with Z<38. For calculations with the ^{78}Ni core a new set of single-particle excitations and the corresponding two-body matrix elements is required, which have been constructed in Ref. [2]. This new set of parameters, after being tested on nuclei with known excitations, could be later used to predict properties of not yet known nuclei in the vicinity of ^{78}Ni and assist their future experimental investigations.

Our studies in the discussed region have begun at its upper-Z end, where nuclei are strongly populated in fission of actinides and some of them can be accessed by reactions on stable targets. Another motivation for studies at Z∼40 was the need to determine single-particle energies of the the $\nu 1h_{11/2}$ neutron and $\pi 1g_{2/2}$ proton excitations. These high-j orbitals, which are expected near the Fermi level at N≈58 and Z≈40, are important for the description of medium- and high-spin levels in spherical nuclei with N<58 and Z<40. Furthermore, the high-j, $\nu 1h_{11/2}$ orbital plays a major role in generating strong quadrupole deformation in nuclei with Z≥38, N∼60 [3–5]. A mechanism explaining the sudden onset of quadrupole deformation around Z=38 and N=60, involves, among other, the crossing of the low-Ω intruder orbitals originating from the $\nu 1h_{11/2}$ subshell with the $\nu 9/2^+[404]$ extruder orbital [6, 7]. Therefore, knowing the positions of these high-j orbitals is vital for a proper description of this deformation onset. The first description using large-scale shell-model calculations has given encouraging results [2].

To date, the energy of the $h_{11/2}$ neutron orbital has not been observed directly. The $11/2^-$ excitations originating from this orbital, expected to be close to the

yrast line in ^{95}Sr or ^{97}Zr, are also not uniquely determined. However, one can study multi-particle configurations involving the $\nu h_{11/2}$ orbital. Excitation energies of such levels are lowered by the attractive interaction of the $h_{11/2}$ neutron with other particles. Examples are the $\nu(g_{7/2}h_{11/2})_{9^-}$ and $(\pi g_{9/2}\nu h_{11/2})_{10^-}$ couplings. Observing such configurations should help determining the position of the high-j $\pi g_{9/2}$ and $\nu h_{11/2}$ orbitals. We note that due to their yrast character such excitations often form isomeric levels with rather simple structures, which are particularly useful for testing shell-model predictions. Until now such configurations have been observed and interpreted in ^{98}Zr [8], ^{97}Y [9], ^{95}Y[10], ^{94,96}Sr [11] and ^{91,93}Rb [12]. We have also proposed two isomers in ^{94}Rb [13], which most likely involve the $\pi g_{9/2}$ and $\nu h_{11/2}$ orbitals.

Based on the systematics of yrast structures in ^{91,93,94,95}Rb [12, 13] one may expect proton-neutron yrast excitations involving the $\pi g_{9/2}$ and $\nu h_{11/2}$ orbitals to be present also in ^{92}Rb. The ^{92}Rb nucleus has been studied in β^- decay of ^{92}Kr [14], where the first excited level at 142.4 keV and several other, low-spin excitations have been reported. Using the 142-keV transition as a gate Hwang et al. [15] have found ten new levels populated in spontaneous fission of ^{252}Cf, which are most likely of yrast character. However, neither spin-parity assignments nor other characteristics of these levels were reported in Ref.[15]. In this situation we reinvestigated yrast excitations in ^{92}Rb in order to obtain more information needed for the interpretation of yrast levels. In Section II of this work we describe our experiments and the data analysis. In Section III the shell-model calculations for ^{92,94}Rb are compared to the experimental results. The work is summarized in Section IV.

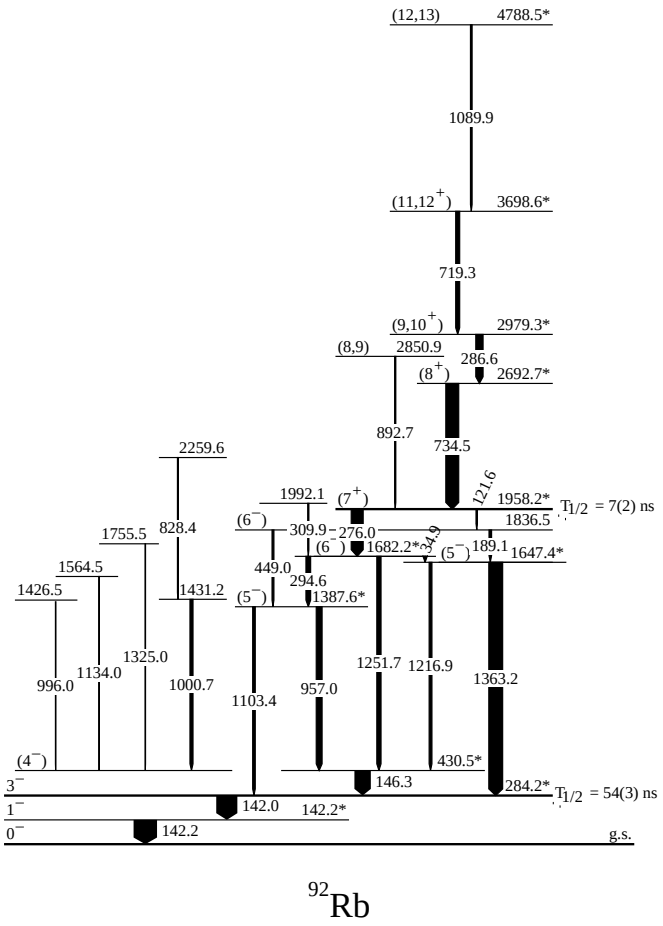

FIG. 1: Level scheme of ^{92}Rb, as obtained in the present work. Excited levels marked with an asterisk have been also reported in [15].

II. EXPERIMENTS AND RESULTS

In our work, excited states in ^{92}Rb have been populated in spontaneous fission of ^{248}Cm and measured by means of γ spectroscopy, using the EUROGAM2 array of Anti-Compton Spectrometers [16]. We have measured high-fold coincidences between γ rays following fission, using a time-coincidence window of 300 ns (more details about this experiment and the data analysis can be found in Ref.[17]). We have also used triple-coincidence data from a measurement of spontaneous fission of ^{252}Cf performed with the GAMMASPHERE detector array. These coincidences, collected with the electronic time-coincidence window of 900 ns, opened by the "start" given by the "Master Gate" signal, have been used to search for isomeric levels in ^{92}Rb (see Ref. [18] for more information on the GAMMASPHERE experiment).

We confirm the excitation scheme reported in Ref.[15]. We note that the transition and level energies reported in Ref.[15] are systematicaly higher than those seen in our work. Consequently, our energies of the higher-lying levels differ by more than a keV from those reported in [15]. To the scheme of Ref.[15] we add seven new levels and a new branching to the 1387.7-keV level (1388.6-keV level in Ref.[15]). We have also identified two new isomers in ^{92}Rb and proposed spins and parities to several levels, as described further in the text. The excitation scheme of ^{92}Rb obtained in this work is drawn in Fig. 1 and in Table I we show properties of gamma transitions in ^{92}Rb, as observed in the present work.

Figures 2 and 3 show two γ spectra measured in fission of ^{248}Cm, which are doubly gated on the 142-142-keV and 276-1363-keV lines, respectively. The spectra were obtained from a $\gamma\gamma\gamma$ histogram sorted with no extra conditions. The spectrum in Fig. 2 shows most of the lines seen in the scheme of ^{92}Rb in Fig. 1 and lines from the complementary Pr isotopes. There are also contaminating lines belonging to ^{96}Sr and ^{148}Ba, which are due to a strong 142 keV lines present in ^{149}Ce, a complementary fission fragment to ^{96}Sr and in ^{148}Ba). The coincidences observed in Fig. 3 require the presence of a low-energy, 34.9-keV transition between the 1682.2- and 1647.4-keV levels. This transition has been also reported in Ref.[15].

TABLE I: Properties of γ transitions in ^{92}Rb, as observed in fission of ^{248}Cm.

E_γ (keV)	I_γ (rel.)	A_2/A_0	A_4/A_0	Correlating E_γ (keV)	Multi-polarity
34.9(2)[a]	40(10)				
121.6(2)	9(2)				
142.0(2)[a]	145(15)	-0.06(1)	-0.01(2)	142.2	ΔI=2
142.2(2)[a]	145(15)	-0.06(1)	-0.01(2)	142.0	ΔI=1[b]
146.3(1)[a]	100(5)	+0.04(2)	+0.32(9)	142.0+142.2	
189.1(2)	16(2)				
276.0(1)[a]	73(5)	+0.11(3)	+0.08(5)	734.5	ΔI=1
286.6(2)[a]	44(4)				
294.6(1)[a]	29(3)				
309.9(2)	21(2)				
449.0(2)	11(2)				
719.3(2)[a]	24(3)				
734.5(2)[a]	70(5)	+0.11(3)	+0.08(5)	276.0	ΔI=1
828.4(3)	6(1)				
892.7(3)	5(1)				
957.0(2)[a]	36(3)	+0.4(1)	+0.03(2)	146.3	
996.0(2)	4(1)				
1000.7(2)	19(2)				
1089.9(4)[a]	10(2)				
1103.4(2)	16(2)				
1134.0(3)	5(1)				
1216.9(2)[a]	17(2)				
1251.7(2)[a]	26(3)				
1325.0(3)	3(1)				
1363.2(2)[a]	84(4)				

[a] also seen in [15]
[b] from [19].

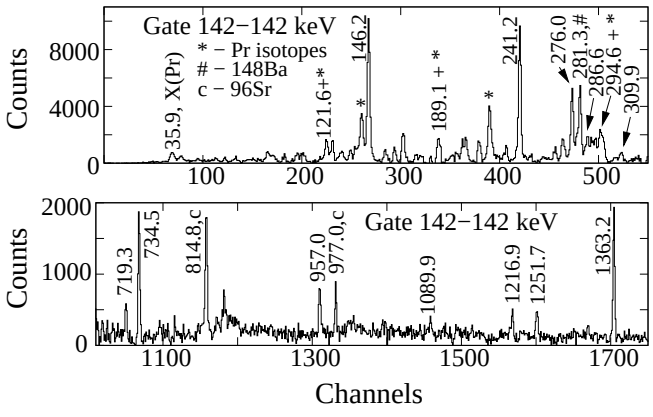

FIG. 2: Coincidence spectrum gated on γ lines in ^{92}Rb, as obtained in this work. Energies of transitions are labeled in keV. Weak, unlabeled lines are contaminations, which could not be identified

In Fig. 2 the 34.9-keV line overlaps with the 35.9-keV, K_α X-ray line of Pr, which is also present in the spectra. However, this doublet could be resolved, using Low Energy Photon Spectrometers (LEPS), four of which were attached to the EUROGAM2 array. Figure 4 displays the low-energy part of a γ spectrum doubly-gated on the

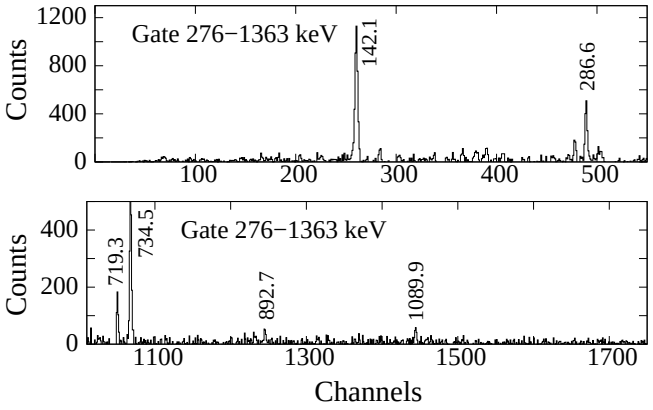

FIG. 3: Coincidence spectrum gated on γ lines in ^{92}Rb, as obtained in this work. Energies of transitions are labeled in keV. Weak, unlabeled lines are contaminations, which could not be identified

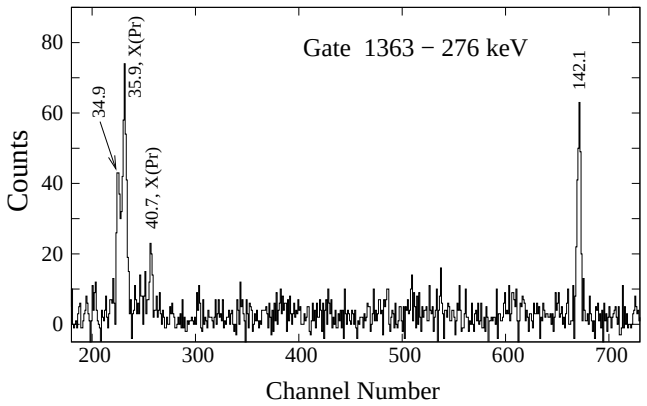

FIG. 4: LEPS coincidence spectrum gated on 1363- and 276-keV γ lines in ^{92}Rb, as obtained in this work. Energies of transitions are labeled in keV.

1363.2- and 276.0-keV lines, which was measured using LEPS. In this spectrum one observes two lines, with energies 34.9 keV and 35.9 keV, the latter line corresponding to the K_α X-rays of Pr (there is also the 40.7-keV, K_β X-ray line of Pr in the spectrum). The 34.9 keV line corresponds to the decay of the 1682.2-keV level.

Figure 5 shows high-energy fragments of further γ coincidence spectra measured in fission of ^{248}Cm, which are doubly gated on the $\gamma\gamma\gamma$ histogram. Figure 5(a) shows two new lines at 892.7 and 1103.4 keV and in Fig. 5(b) a new line at 828.4 keV is seen. These lines, although present in Fig. 2(a), are not clearly visible there due to a larger scale and higher background fluctuations. Similarly, a clean double gate on the $\gamma\gamma\gamma$ histogram, shown in Fig. 6, where the first gate is set on the 957-keV line and the second gate on both, 146-keV and 295-keV lines, reveals a new line at 309.9 keV (seen also in Fig. 2).

In Figs. 7 and 8 we show coincidence spectra doubly gated on the 142-146 keV and 142-1363 keV lines, respectively. In Fig. 7 there is a new line at 449.0 keV and in Fig. 8 two new lines, at 121.6 keV and 189.1 keV (seen

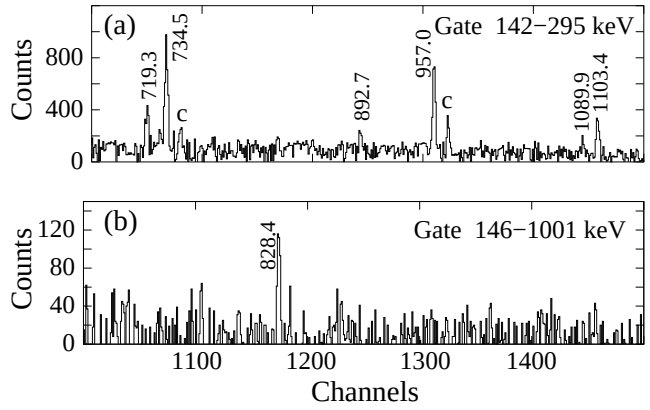

FIG. 5: Coincidence spectra gated on γ lines in ^{92}Rb, as obtained in this work. Energies of transitions are labeled in keV. Label "c" denotes unidentified contaminating lines.

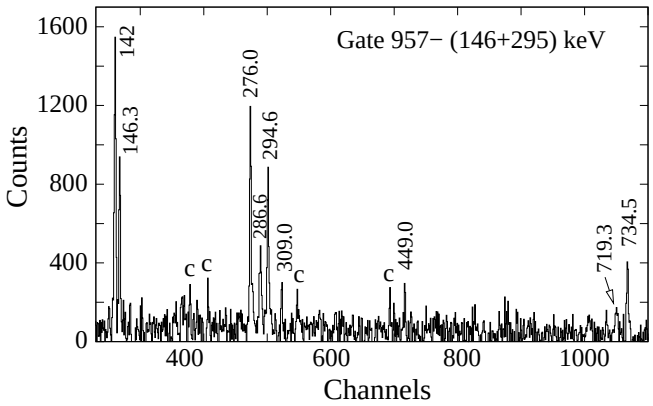

FIG. 6: Coincidence spectra gated on γ lines in ^{92}Rb, as obtained in this work. Energies of transitions are labeled in keV. Label "c" denotes unidentified contaminating lines.

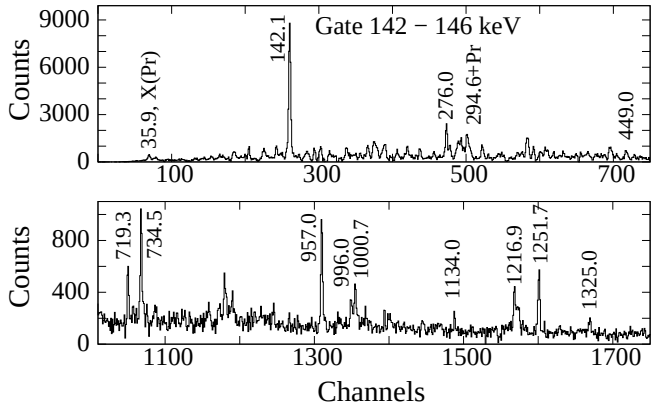

FIG. 7: Coincidence spectrum gated on γ lines in ^{92}Rb, as obtained in this work. Energies of transitions are labeled in keV.

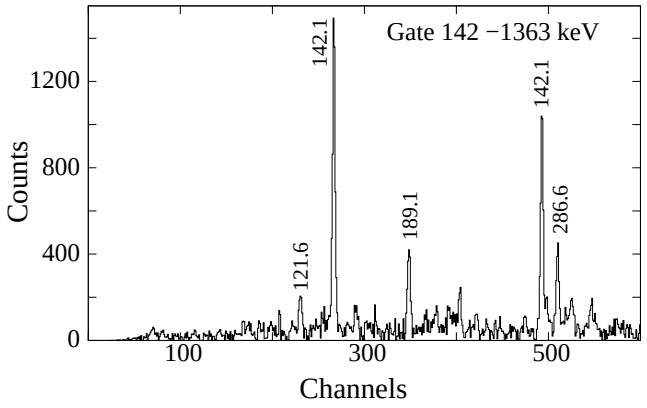

FIG. 8: Coincidence spectrum gated on γ lines in ^{92}Rb, as obtained in this work. Energies of transitions are labeled in keV.

also in Fig. 2). These three lines establish a new level at 1836.5 keV and confirm the energy spacing between the 1647.4- and 1958.2-keV levels, supporting the presence of the 34.9 keV transition.

To search for isomeric levels in ^{92}Rb we have sorted the coincidence data from the fission of ^{252}Cf into histograms with various conditions on time signals, as described in detail in Ref.[10]. Into these histograms we sorted prompt, p, γ rays registered within the period from -10 ns to +10 ns relative to the "0" time given by the Master-Gate signal of GAMMASHEPRE as well as delayed, d, γ rays, registered within the period from 40 ns to 210 ns after the "0" time. It should be noted that the Master-Gate signal was generated when a three- or higher-fold coincidence was registered. The "0" time corresponds to the arrival time of the first γ in such a coincidence event. Consequently, when γ rays in a coincidence event correspond to transitions below and above an isomer, their time signals are different, allowing the identifiation of an isomer.

A two-dimensional histogram, *dp* matrix, has been sorted out of pairs delayed-prompt γ-γ coincidence events and another histogram, *dd* matrix, has been sorted out of pairs γ-γ coincidence events, where both γ rays were delayed. Figure 9 shows two γ spectra obtained from these two matrices by gating on the 142-keV delayed line. The spectrum in Fig. 9(a), obtained from the *dd* matrix, is dominated by the 142-keV line while in the spectrum in Fig. 9(b), obtained from the *dp* matrix only lines feeding the 284.2 keV level are seen. This shows that both lines in the 142.2-142.0 keV cascade are delayed while lines above the 284.2 keV level have prompt components. Therefore, we conclude that the 284.2 keV level is an isomer with a half life in the nanosecond range.

Although lines above the 284.2 keV level show prompt feeding, they may also have delayed components. In Fig. 10 we show a spectrum obtained by gating on the delayed 1363.2-keV line in the *dp* matrix. In the spectrum one observes the 734.5- and 286.6-keV lines, which are prompt with respect to the 1363.2-keV line. The 276.0-keV line is not present here, while it is clearly seen in Fig.9(b). This indicates that the 1958.2-keV level is also an isomer.

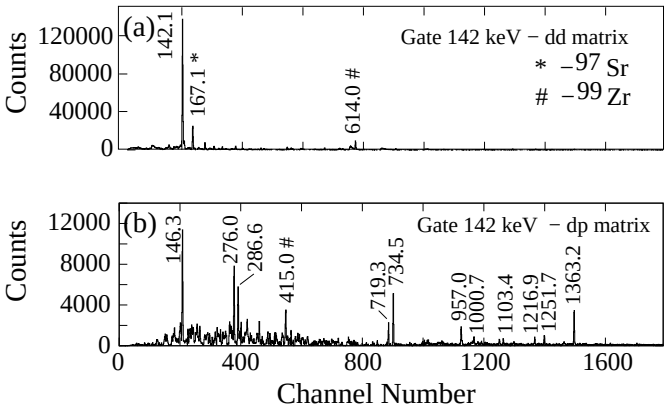

FIG. 9: Coincidence spectra gated on γ lines in ^{92}Rb, as obtained in this work. Energies of transitions are labeled in keV.

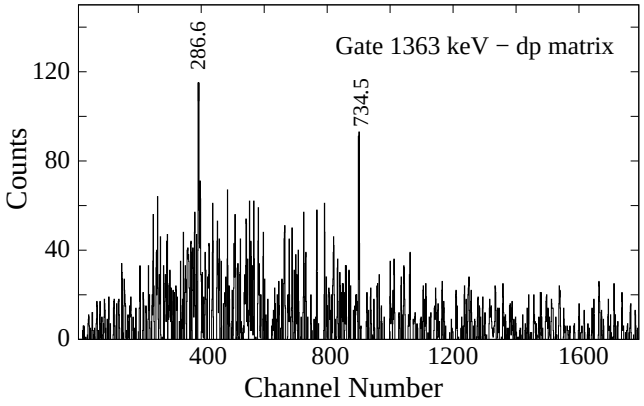

FIG. 10: A coincidence spectrum gated on the 1363 keV γ line in ^{92}Rb, as obtained in this work. Energies of transitions are labeled in keV.

The "dual" nature of the 1363.2-keV line seen in Fig. 9(b) as prompt and being a delayed gate in Fig. 10 is due to the fact that the 1647.4 keV level receives both the prompt feeding from fission and a delayed feeding from the decay of the 1958.2-keV isomer. Analogously, the 276.0-keV line is seen in Fig. 9(b) because the 142-keV doublet is delayed relative to it, while it is not seen in in Fig. 10 because the 1363.2-keV line is not delayed relative to it.

These time correlations are further confirmed by doubly-gated γ-spectra obtained from three-dimensional histograms (cubes). We sorted a cube called *ddp* out of triple-γ coincidences, where prompt γ energy has been sorted along the p axis, and two delayed γ energies have been sorted along the two d axes. Figure 11(a) shows a spectrum doubly-gated on the delayed 142- and 276.0-keV lines, in which only lines above the 1958.2-keV level are seen (there is no 1363.2-keV line). Figure 11(b) shows a spectrum doubly-gated on the delayed 276.0- and 1363.2-keV lines. Here also only lines above the 1958.2-keV level are seen.

Using the ^{252}Cf fission data we could determine the

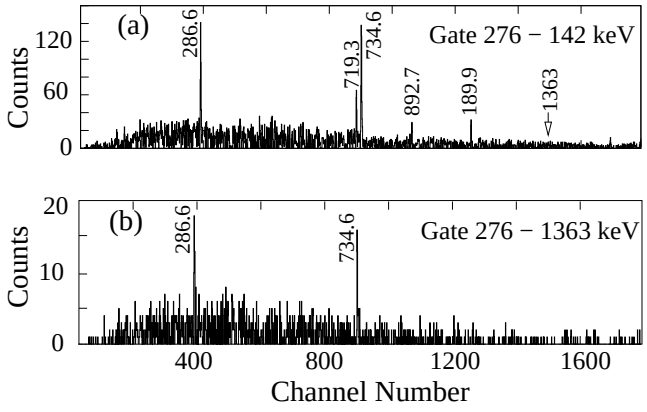

FIG. 11: Coincidence spectra from the *ddp* cube, gated on γ lines in ^{92}Rb, as obtained in this work. Energies of transitions are labeled in keV.

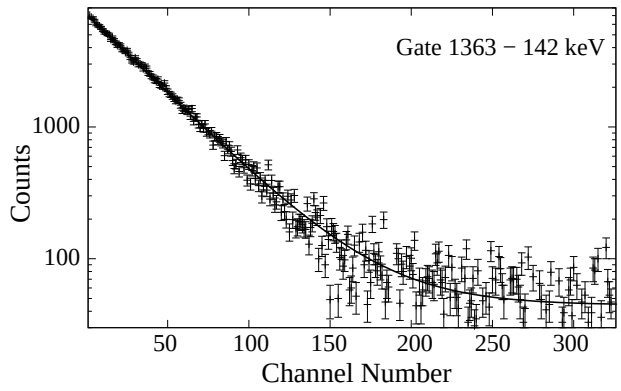

FIG. 12: A time spectrum double gated on the 1363.2-keV prompt line and lines depopulating the 284.2-keV isomer in ^{92}Rb, as seen in the ^{252}Cf data. Time calibration is 2.2 ns per channel. The solid line represents a fit of an exponential decay plus a constant background.

half-life of the 284.2-keV isomer from the time-decay spectrum corresponding to 142-keV transitions depopulating this isomer. The spectrum was cut out of the *pgt* cube where we sorted along the p axis γ signals registered within the "prompt" time window, along the g axis all γ signals (no time condition) and along the t axis time values corresponding to the γ signals sorted to the g axis. In the *pgt* cube we set a prompt-γ gate on the 1363.2-keV line feeding the 284.2-keV isomer while on the g axis we gated the 142-keV doublet. The resulting time spectrum is shown in Fig. 12. An exponential decay plus constant background fitted to this time spectrum provided a half-life of $T_{1/2}$=54(3) ns for the 284.2-keV isomer in ^{92}Rb.

Similarly, by gating on the 734.5 keV prompt line above the 1958.2-keV isomer and the 276.0- and 1363.2-keV lines below it, we obtained a time-decay spectrum corresponding to the 276.0- and 1363.2-keV transitions depopulating the 1958.2 keV isomer. An exponential decay plus constant background fitted to these time spectra

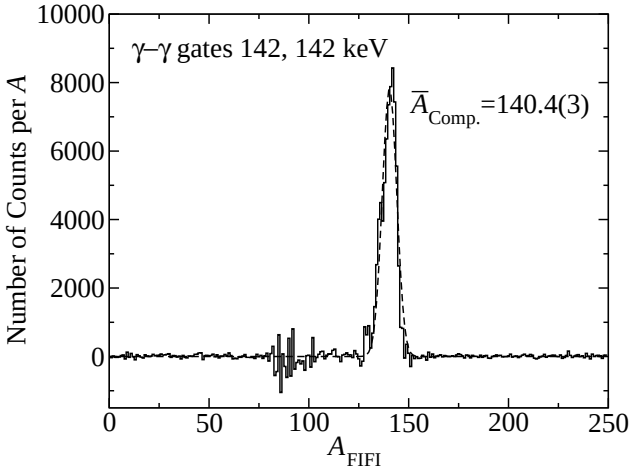

FIG. 13: Mass spectrum of complementary fission fragment gated on the 142-keV delayed line as measured following neutron-induced fission of ^{235}U using the FIFI detector. See text for further explanation.

provided a half-life of $T_{1/2}$=7(2) ns for the 1958.2-keV isomer in ^{92}Rb.

The presence of the 284.2-keV isomer in ^{92}Rb has been further confirmed in another measurement, performed at the cold-neutron beam facility PF1B [20] of the Institute Laue-Langevin, Grenoble, where we measure delayed γ rays following fission of ^{235}U induced by thermal neutrons. In the experiment fission fragments could escape the target and fly to the stopper foil placed at 70 cm from the target. There, delayed γ rays from the stopped fragments were measured by an array of 15 Ge detectors. The complementary fragment was detected in the fission fragment detector FIFI [21], used to determine the mass of the fragment. More details on this experiment are given in Refs.[12, 13]. Figure 13 displays a mass spectrum measured by FIFI, $A_{\rm FIFI}$, where a coincidence with two γ rays of 142-keV energy measured in Ge detectors was required. The peak in the spectrum at mass $A_{Comp.}$=140.4(3) corresponds to the average mass of the fission fragment complementary to the fragment emitting 142-keV delayed lines. Using the mass calibration of FIFI [12] we deduced the mass of the fragment emitting 142-keV delayed lines to be 92.1(3), which confirms the assignment of the 142.2-142.0 keV γ cascade to ^{92}Rb.

Spin and parity assignments are crucial for the interpretation of nuclear states. We have obtained angular correlations for a few γ-γ cascades in ^{92}Rb observed in the ^{248}Cm fission experiment, using techniques developed in Refs. [22, 23]. The resulting experimental angular-correlation coefficients are shown in Table I. Except for the 142.2-keV line, there are no other stretched transitions known in ^{92}Rb. Therefore, the angular correlations alone are not fully conclusive. When proposing spins to levels in ^{92}Rb we have used, in addition, arguments based on decay branchings and half-lives as well as on the known fact [24] that the fission process populates predominantly yrast states.

In β^- decay of ^{92}Kr [14], the ground state and the first excited level at 142.2 keV were tentatively assigned spin and parity $(1^-)$and (2^-), respectively. The spin and parity of the ground state has been later determined to be 0^- [25, 26]. Consequently, because of an M1+E2 multipolarity of the 142.2-keV transition the 142.2-keV level was assigned spin and parity 1^- [19].

With the ΔI=1 character of the 142.2-keV transition, our angular correlations for the 142.0-142.2 keV cascade indicate a stretched quadrupole character for the 142.0-keV transition. The halflife of the 284.2-keV level is consistent with an E2 rather than M2 character of the 140.0-keV transition, hence a spin and parity of $I^\pi=3^-$ can be assigned to the 284.2-keV level. We note that the non-observation of any decay branch of the 284.2-keV level to the ground state is consistent with the $I^\pi=3^-$ assignment for the 284.2-keV level.

The upper limit for a halflife of the 430.5-keV level is 5 ns in our measurement. This is not consistent with a stretched quadrupole multipolarity for the 146.3-keV transition. Consequently spin 5 for the 430.5-keV level is a less likely solution. Because the 430.5-keV level does not decay to the 142.2-keV level, its spin and parity is limited to either $I^\pi=3^+$ or I=4. Low energy excitations in ^{92}Rb correspond to proton-neutron configurations, where the neutron can occupy one of the $d_{5/2}$, $g_{7/2}$ or $s_{1/2}$ orbitals, all of positive parity, and the proton can occupy the $f_{5/2}$ or $p_{1/2}$ orbital, both of negative parity. To produce a positive-parity proton-neutron level in ^{92}Rb would require placing the odd proton on the $g_{9/2}$ orbital. However, this orbital is much higher in energy. The $9/2^+$ excitation in ^{91}Rb is at 1134 keV above the $3/2^-$ ground state. One also does not expect any octupole excitation at 430 keV in this region of nuclei. Therefore we conclude that the positive parity for the 430.5-keV level is unlikely and propose spin and parity $I^\pi=(4^-)$ for this level. The angular correlation of the 146.3-keV line with the 142.1-keV doublet does not contradict this proposition.

The next group of levels populated in ^{92}Rb appears about 1 MeV above the 430.5-keV level. One expects spins higher than 4 for these levels, considering that the fission process populates levels close to the yrast line. Therefore, taking into account the observed branching we propose spin and parity $I^\pi=(5^-)$ for the 1387.6- and 1647.4-keV levels.

Due to its prompt character the 34.9-keV line can not correspond to a ΔI=2 spin change. Therefore, possible spins for the 1682.2-keV level are I=5 or I=6. The $I^\pi=5^+$ is less likely because then the B(E1;34.9-keV)/B(E1;1251.7-keV) branching would be at odds with the Alaga rules. The $I^\pi=5^-$ solution is also less likely because there is no decay from the 1958.2-keV level to the 1647.4-keV level, while there is a strong decay branch to the 1682.2-keV level. Therefore we propose spin I=6 for the 1682.2-keV level. Again, the positive parity and, consequently, E1 multipolarities for the 34.9- and 294.6-keV transitions depopulating the 1682.2-keV level would

strongly violate the Alaga rules. Therefore we propose negative parity for the 1682.2-keV level.

The lack of decay from the 1958.2-keV level to the 1647.4-keV level and the strong 276.0-keV decay branch to the 1682.2-keV suggest spin and parity $I^{\pi}=7^{+}$ or $I^{\pi}=8$ for the 1958.2-keV level. The $I^{\pi}=8^{+}$ is unlikely, considering the halflife of the 1958.2-keV level. This halflife of the 1958.2-keV level is consistent with an E1 multipolarity for the 276.0 keV transition and, therefore, spin and parity $I^{\pi}=7^{+}$ for the 1958.2-keV level.

The yrast-population argument suggests that the spin of the 1836.5-keV level is lower than the spin of the 1958.2-keV level. We propose spin and parity $I=6^{-}$ for the 1836.5-keV level because of the prompt character of the 189.1-keV decay and the decay branchings observed for the 1958.2-keV level.

The angular correlation for the 276.0-734.5-keV cascade is consistent with both transitions in the cascade corresponding to a $\Delta I=1$ spin change (it is clearly not a stretched dipole-quadrupole solution). Therefore we propose spin 8 for the 2692.7-keV level. Positive parity is preferred because no decays to levels with spin 6 are seen.

For the 2850.9-, 2979.3-, 3698.6- and 4788.5-keV levels we propose spins and parities as shown in Fig. 1, based on the yrast-population argument and the observed decay branches.

The above spin and parity assignments proposed for levels in ^{92}Rb are tentative for most cases. Therefore they are placed in parenthesis. We note, though, that they are consistent with all the experimental observations known for ^{92}Rb.

The halflives of isomers in ^{92}Rb can be used to estimate transition rates in this nucleus. From the $T_{1/2}$ = 54(3) ns halflife of the 284.2-keV level we deduced the B(E2) rate of 7.2(4) W.u. for the 142.0-keV E2 transition. This value is typical for spherical nuclei in this region (^{93}Kr, ^{91,93}Rb, ^{92,94}Sr, ^{94,96}Zr [27]). Similarly, from the $T_{1/2}$ = 7(2) ns halflife of the 1958.2-keV level we deduced the B(E1) transition rate of the 276.0-keV E1 transition to be $2.3(7)\times10^{-6}$ W.u., a value similar to the B(E1)=$3.8(3)\times10^{-6}$ W.u. transition rate of the 169-keV E1 transition depopulating the 18 ns isomer at 1485.2 keV in ^{94}Rb. Both B(E1) values are typical single-particle E1 rates observed in medium-mass nuclei. We note that these values do not indicate any enhanced octupole correlations in ^{92,94}Rb.

III. DISCUSSIONS

Isomeric levels observed in ^{92}Rb and ^{94}Rb [13] may serve as yet another test of large scale shell-model calculations with the ^{78}Ni core. After a rather successful reproduction of excitations in odd-A nuclei, such as ^{91,93}Rb [12] or ^{95}Y [10], isomeric levels observed in odd-odd nuclei should provide a more specific test of the proton-neutron coupling and the corresponding matrix elements.

Let us first briefly summarize on what are the expected dominating configurations in ^{92}Rb near the yrast line. Orbitals, which should form near-yrast excitations in ^{92}Rb are the $d_{5/2}$, $g_{7/2}$ and $h_{11/2}$ neutrons and $p_{3/2}$, $f_{5/2}$ and $g_{9/2}$ protons. In the odd-A neighbors, ^{91}Rb and ^{91}Kr, the ground states have spins and parities of $3/2^{(-)}$ and $5/2^{(+)}$, most likely corresponding to the $\pi p_{3/2}$ and $\nu d_{5/2}$ single-particle configurations, respectively. These levels may form in ^{92}Rb a multiplet of low-lying levels with spins 1^{-}, 2^{-}, 3^{-} and 4^{-}. There are also low-energy excitations in the odd-A neighbours, the $5/2^{(+)}$ level at 108.8 keV in ^{91}Rb and a level at 144.6 keV in ^{91}Kr, having spin $(3/2^{+})$. These low-energy levels can couple with the corresponding ground states to produce low-lying 0^{-} and 5^{-} levels in ^{92}Rb.

The next group of near yrast levels with spins 4, 5 and 6 and negative parity is expected in ^{92}Rb when the odd neutron is promoted to the $g_{7/2}$ orbital and couples to the $\pi p_{3/2}$ and $\pi f_{5/2}$ low-energy levels of ^{91}Rb. Unfortunately, little is known about yrast excitations in ^{91}Kr [28] (in ^{93}Sr, which has also N=55 neutrons, a probable $7/2^{+}$ level is reported at 1238 keV [29], which could correspond to the $\nu g_{7/2}$ configuration).

In ^{91}Rb the $9/2^{+}$ level, which may have a contribution from the $\pi g_{9/2}$ configuration in its wave function, is seen at 1134 keV [15]. Therefore in ^{92}Rb one may expect an yrast level with spin and parity 7^{+}, corresponding to the coupling of the $d_{5/2}$ neutron with the proton promoted to the $\pi g_{9/2}$ orbit. We note, that in ^{94}Rb, where the $d_{5/2}$ subshell is filled and the valence neutron is expected to be in the $\nu g_{7/2}$ orbit, the $(\pi g_{9/2}\otimes\nu d_{5/2})_{7^{+}}$ configuration is not expected at the yrast line. Instead, an 8^{+} level should appear, which may have lower excitation energy than the 7^{+} level in ^{92}Rb, because the $(\pi g_{9/2}\otimes\nu g_{7/2})_{8^{+}}$ coupling is expected to be more attractive than the $(\pi g_{9/2}\otimes\nu d_{5/2})_{7^{+}}$ coupling, due to a larger overlap of the $\nu g_{7/2}$ and $\pi g_{9/2}$ wave functions.

Higher-energy and higher-spin levels in ^{92}Rb and ^{94}Rb can be formed when the valence proton and neutron are both promoted to higher-lying orbitals $\pi g_{9/2}$, $\nu g_{7/2}$ or $\nu h_{11/2}$, respectively. A level with spin and parity 8^{+} is expected in ^{92}Rb corresponding to the $(\pi g_{9/2}\otimes\nu g_{7/2})_{8^{+}}$ configuration. Because both nucleons are promoted, the excitation energy of the 8^{+} level in ^{92}Rb should be higher than the excitation energy of the 8^{+} in ^{94}Rb.

Further up, the $(\pi g_{9/2}\otimes\nu h_{11/2})_{10^{-}}$ configuration is expected near the yrast in both, ^{92}Rb and ^{94}Rb, though it may have lower excitation energy in ^{94}Rb due to a lower energy, relative to the Fermi level, of the $\nu h_{11/2}$ orbital at N=57 as compared to its energy at N=55.

To verify these expectations we have performed shell-model calculations for ^{92}Rb and ^{94}Rb isotopes, using a large valence space based on the ^{78}Ni core, including $(1f_{5/2}, 2p_{1/2}, 2p_{3/2}, 1g_{9/2})$ orbitals for protons and $(2d_{5/2}, 3s_{1/2}, 2d_{3/2}, 1g_{7/2}, 1h_{11/2})$ for neutrons. The effective interaction used in this work was derived by the monopole corrections of the realistic G-matrices based on

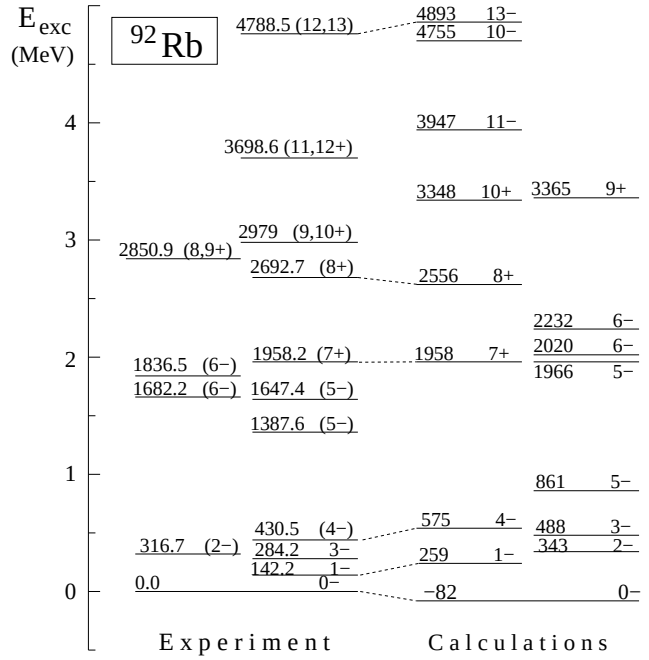

FIG. 14: Comparison of experimental excitation energies in ^{92}Rb to the shell-model calculations performed in this work. See text for further explanation.

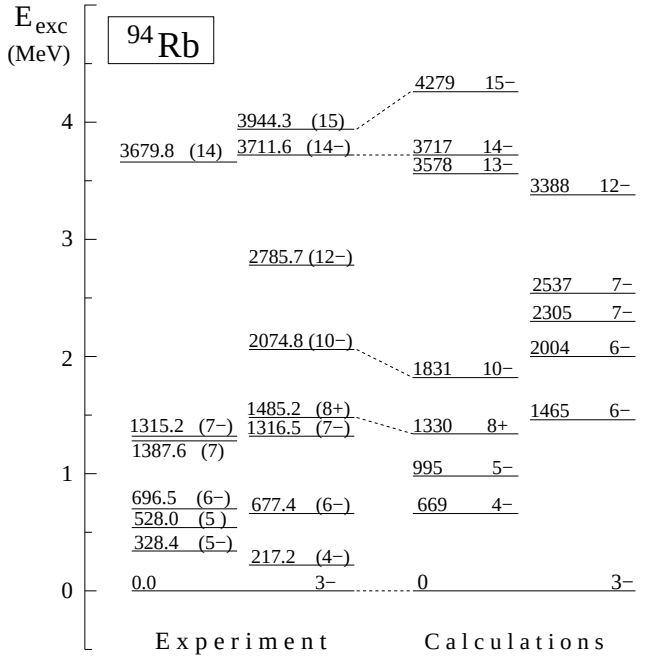

FIG. 15: Comparison of experimental excitation energies in ^{94}Rb to the shell-model calculations performed in this work. See text for further explanation.

the CD-Bonn potential. A broader discussion of the interaction and its other applications can be found in [2]. We also refer the reader to our recent work [12], where analogous shell model calculations have been performed for odd-A Rb isotopes.

The truncated shell-model calculations for ^{92,94}Rb were performed with the code ANTOINE [30]. We pursued the calculations up to the 8p8h level with respect to the $\pi(p_{3/2})\nu(d_{5/2})$ shell closures in ^{92}Rb and up to 6p6h in ^{94}Rb, with no additional constraints on the occupancies of valence orbitals. In such a scheme the largest dimensions do not exceed 8×10^9 and the low-lying levels are reasonably converged.

The excitation energies calculated for ^{92}Rb are compared to the experimental excitation energies in Fig. 14. In the experimental set we included the 316.7-keV level seen in β decay [14], which is a good candidate for the 2^- excitation in ^{92}Rb. The experimental and calculated levels have been, arbitrarily, normalized to each other at the 1958.2-keV, 7^+ level.

The overall reproduction of the experimental data is good, considering the complex nature of this odd-odd nucleus with 14 valence nucleons in the model space. The key excitations, the ground state, the two isomers and the 8^+ level are reproduced within 100 keV, which is better than an average accuracy for the large-scale shell-model calculations. The model reproduces well the multiplet of 0^- - 4^- low energy levels and the group of 5^- and 6^- excitations, though the latter are about 400 keV higher than in the experiment. The largest discrepancy is seen for the first 5^- excitation, which is calculated well below the experimental candidate. As discussed above, a low-energy $(\pi f_{5/2} \otimes \nu d_{5/2})_{5^-}$ configuration may be expected in ^{92}Rb, however, such a level is not seen in our data. It is unlikely that it is a long-lived isomer located near the ground state, which has escaped detection because of a long halflife. In such a case one should see decays to this isomer from higher lying levels with spins 5 and 6. A possible explanation is that low-energy levels in the neighboring ^{91}Kr are more collective than expected. Their structure, which is poorly known, should be investigated.

It is interesting to inspect the occupation of valence neutron and proton orbitals as calculated in this work for levels in ^{92}Rb. The corresponding numbers are shown in Table II. For the 0^- and 3^- levels the occupation of valence orbitals is similar. These levels are formed primarily by coupling of the $d_{5/2}$ neutron to $p_{1/2}$ and $p_{3/2}$ protons (though an admixture of the $s_{1/2}$ neutrons is present). For the 7^+ level one proton is promoted to the $g_{9/2}$ orbital and for the 8^+ level, in addition, a neutron is promoted to the $g_{7/2}$ orbital, in agreement with the expectations outlined above. We note that the calculated occupation of the $h_{11/2}$ neutron orbital for the 10^- is rather low, which explains the high excitation energy of this state, calculated at 4755 keV. The non-observation of this level in ^{92}Rb, in the experiment, is probably due to its too non-yrast character.

In our work on ^{94}Rb [13] we have proposed proton-neutron dominating configurations for the yrast levels in ^{94}Rb. In Fig. 15 we compare the experimental levels in ^{94}Rb [13] with the shell-model calculations, performed

TABLE II: Occupation of orbitals, as calculated in this work for levels in ^{92}Rb.

	0^- -82-keV	3^- 343-keV	7^+ 1958-keV	8^+ 2556-keV	10- 4755-keV
neutrons					
$d_{5/2}$	4.22	4.11	3.67	3.04	3.59
$s_{1/2}$	0.33	0.41	0.66	0.42	0.56
$g_{7/2}$	0.10	0.12	0.17	0.99	0.15
$d_{3/2}$	0.19	0.22	0.35	0.39	0.41
$h_{11/2}$	0.15	0.15	0.16	0.15	0.29
protons					
$f_{5/2}$	4.66	4.60	4.15	4.17	4.24
$p_{3/2}$	3.12	3.07	2.76	2.77	2.80
$p_{1/2}$	0.87	1.01	0.90	0.84	0.91
$g_{9/2}$	0.36	0.32	1.19	1.22	1.04

in the present work, with 16 valence particles, the most complex shell-model investigation in this region. The 4 MeV scale of the observed excitations is reproduced well and again the ground state and the two isomers are reproduced closely by the calculations, supporting their proposed structures. In the 8^+ state wave function, the total occupation of the $\pi g_{9/2}$ orbital is equal to 1.12 and that of the $\nu g_{7/2}$ orbital is equal to 1.05, with nearly no particle (0.13) in the $\nu h_{11/2}$ orbital, as expected. The contrary is found for the 10^- level, where the proton wave function is very similar to that of the 8^+ state with 1.11 particle in the $\pi g_{9/2}$ but with 1.07 neutron now located in the $\nu h_{11/2}$ orbital and the $\nu g_{7/2}$ orbit emptied (0.11).

Compared to the 10^- level in ^{92}Rb, the increased occupation of the $\nu h_{11/2}$, results in a much lower excitation energy of the 10^- level, which becomes yrast, and strongly populated in fission. The lowering of the excitation energy is primarily due to the strongly attractive interaction between $\pi g_{9/2}$ protons and $h_{11/2}$ neutrons. The calculations reproduce also the characteristic observation that the 8^+ level in ^{94}Rb is about 1 MeV lower than in ^{92}Rb and that there is no 7^+ yrast level in ^{94}Rb.

The fair reproduction in ^{94}Rb of the 8^+ and 10^- levels, as well as the 15^- level, based on the $(\pi g^1_{9/2} \otimes \nu g^1_{7/2} h^1_{11/2})_{15^-}$ structure, confirms that the proton-neutron $g_{9/2}$-$g_{7/2}$ and $g_{9/2}$-$h_{11/2}$ monopoles are correctly constrained in the present interaction.

The levels with spins 4^- to 7^- in ^{94}Rb are calculated well above their experimental counterparts. These states are sensitive to the pf-$g_{7/2}$ monopoles, for which no clear experimental constraint is yet available. Little is known about the nature of the $7/2^+$ states in the $N = 51$ isotones below $Z = 40$ [31]. Experimental and theoretical work in progress [32] may provide this missing benchmark for future shell model calculations with the ^{78}Ni core.

IV. SUMMARY

The near-yrast, medium-spin excitations in the neutron-rich, odd-odd nucleus ^{92}Rb have been studied experimentally via neutron-induced and spontaneous fission reactions. The combination of the data from delayed and prompt γ-ray spectroscopy experiments using the EUROGAM2 and GAMMASPHERE Ge arrays and the FIFI spectrometer allowed the unique identification of two new isomers in ^{92}Rb and a construction of a scheme of excited levels with tentative spin and parity assignments. The experimental data obtained for ^{92}Rb and those obtained earlier for ^{94}Rb, have been interpreted using large-scale shell-model calculations. The comparison of the experimental and theoretical results allowed further testing of single-particle energies outside the ^{78}Ni core and in particular the positions of the $\nu h_{11/2}$ orbital forming a characteristic $(\pi g_{7/2} \nu h_{11/2})_{10^-}$ excitation in ^{94}Rb. The shell model calculations reproduce well excitation energies of all four isomers found in ^{92}Rb and ^{94}Rb. The overall reproduction of excited levels is good in ^{92}Rb but in ^{94}Rb the experimental levels with spins 4^- to 7^- are well below the calculations, pointing to the need for further experimental and theoretical efforts.

This work has been supported by the Polish MNiSW grant Nr. N N202 007334 and by the U.S. Department of Energy, Office of Nuclear Physics, under contract No. DE-AC02-06CH11357. The authors are indebted for the use of ^{248}Cm to the Office of Basic Energy Sciences, Dept. of Energy, through the transplutonium element production facilities at the Oak Ridge National Laboratory. We would like to thank M.P. Carpenter, R.V.F. Janssens, F.G. Kondev, T. Lauritsen, C.J. Lister and D. Seweryniak of the Physics Division of Argonne National Laboratory for their help in preparing and running the GAMMASPHERE measurement. Discussions with F. Nowacki are greatfully acknowledged.

[1] A. Holt, T. Engeland, M. Hjorth-Jensen, and E. Osnes, Phys. Rev. C **61**, 064318 (2000).
[2] K. Sieja, F. Nowacki, K. Langanke, and G. Martínez-Pinedo, Phys. Rev. C **79**, 064310 (2009).
[3] T. Werner, J. Dobaczewski, M.W. Guidry, W. Nazarewicz, and J.A. Sheikh, Nucl. Phys. **A 578**, 1 (1994).
[4] J. Skalski, S. Mizutori, and W. Nazarewicz, Nucl. Phys. **A 617**, 282 (1997).
[5] W. Urban, J.L. Durell, A.G. Smith, W.R. Phillips, M.A. Jones, B.J. Varley, T. Rząca-Urban, I. Ahmad, L.R.Morss, M. Bentaleb, and N. Schultz, Nucl. Phys. **A 689**, 605 (2001).
[6] W. Urban , J.A. Pinston, T. Rząca-Urban, A. Złomaniec, G. Simpson, J.L. Durell, W.R. Phillips, A.G. Smith, B.J. Varley, I. Ahmad, N. Schulz, Eur. Phys. J A 16, 11 (2003)
[7] W. Urban, J.A. Pinston, J. Genevey, T. Rząca-Urban, A.

Złomaniec, G. Simpson, J.L. Durell, W.R. Philips, A.G. Smith, B.J. Varley, I. Ahmad, and N. Schulz, Eur. Phys. J. A **22**, 241 (2004).
[8] G.S. Simpson, J.A. Pinston, D. Balabanski, J. Genevey, G. Georgiev, J. Jolie, D.S. Judson, R. Orlandi, A. Scherillo, I. Tsekanovich, W. Urban, and N. Warr, Phys. Rev. C **74**, 064308 (2006).
[9] G. Lhersonneau, D. Weiler, P. Kohl, H. Ohm, K. Systemich, and R.A.Meyer, Z. Phys. A **323**, 59 (1986).
[10] W. Urban, K. Sieja, G. S. Simpson, H. Faust, T. Rząca-Urban, A. Złomaniec, M. Łukasiewicz, A. G. Smith, J. L. Durell, J.F. Smith, B. J. Varley, F. Nowacki, and I. Ahmad, Phys. Rev. C **79**, 044304 (2009).
[11] T. Rząca-Urban, K. Sieja, W. Urban, F. Nowacki, J. L. Durell, A. G Smith, and I. Ahmad, Phys. Rev. C **79**, 024319 (2009).
[12] G. S. Simpson, W. Urban, K. Sieja, J. A. Dare, J. Jolie, A. Linnemann, R. Orlandi, A. Scherillo, A. G. Smith, T. Soldner, I. Tsekhanovich, B. J. Varley, A. Złomaniec, J. L. Durell, J. F. Smith, T. Rząca-Urban, H. Faust, I. Ahmad, and J. P. Greene, Phys. Rev. C **82**, 024302 (2010).
[13] I. Tsekhanovich, G. S. Simpson, W. Urban, J. A. Dare, J. Jolie, A. Linnemann, R. Orlandi, A. Scherillo, A. G. Smith, T. Soldner, B. J. Varley, T. Rząca-Urban, A. Złomaniec, O. Dorvaux, B. J. P. Gall, B .Roux, and J. F. Smith, Phys. Rev. C **78.**, 011301(R) (2008).
[14] R. J. Olson, W. L. Talbert, Jr., and J. R. McConnel, Phys. Rev. C **5**, 2095 (1972).
[15] J. K. Hwang, A. V. Ramayya, J. H Hamilton, S. H. Liu, K. Li, H. L. Crowell, C. Goodin, Y. X. Luo, J.O. Rasmussen, and S. J. Zhu, Phys. Rev. C **80**, 037304 (2009).
[16] P.J. Nolan, F.A. Beck, and D.B. Fossan, Ann. Rev. Nucl. Part. Sci.**44**, 561 (1994).
[17] W. Urban, J.L. Durell, W.R. Phillips, A.G. Smith, M.A. Jones, I. Ahmad, A.R. Barnet, S.J. Dorning, M.J. Leddy, E. Lubkiewicz, L.R. Morss, T. Rząca-Urban, R.A. Sareen, N. Schulz, and B.J. Varley, Z. Phys.A **358**, 145 (1997).
[18] D. Patel, A.G. Smith, G.S. Simpson, R.M. Wall, J.F. Smith, O.J. Onakanmi, I. Ahmad, J.P. Greene, M.P. Carpenter, T. Lauritsen, C.J. Lister, R.F. Janssens, F.G. Kondev, D. Seweryniak, B.J.P. Gall, O. Dorveaux, and B. Roux, J. Phys. G. Nucl. Part. Phys. **28**, 649 (2002).
[19] C. M. Baglin, Nucl. Data. Sheets **91**, 423 (2000).
[20] H. Abele, D. Dubbers, H. Häse, M. Klein, A. Knöpfler, M. Kreuz, T. Lauer, B. Märkisch, D. Mund, V. Nesvizhevsky, A. Petoukhov, C. Schmidt, M. Schumann, and T. Soldner, Nucl. Intr. Meth. A **562**, 407 (2006).
[21] C. J. Pearson, B. J. Varley, W. R. Phillips, and J. L. Durell, Rev. Sci. Instrum.**66** 3367 (1995).
[22] W. Urban, M.A. Jones, C.J. Pearson, I. Ahmad, M. Bentaleb, J.L. Durell, M.J. Leddy, E. Lubkiewicz, L.R. Morss, W.R. Phillips, N. Schulz, A.G. Smith, B.J. Varley, Nucl.Instr.Meth. A 365, 596 (1995)
[23] M.A. Jones, W. Urban, and W.R. Phillips, Rev.Sci.Instrum. **69**, 4120 (1998).
[24] I. Ahmad and W.R. Phillips, Rep. Prog. Phys. **58**, 1415 (1995).
[25] C. Ekstrom, L. Robertsson, G. Wannberg, and J. Heinemeier, Phys. Scr. **19**, 516 (1979).
[26] C. Thibault, *et al.*, Phys. Rev. C **23**, 2720 (1981).
[27] Evaluated Nuclear Structure Data File (www.nndc.bnl.gov), (2011).
[28] J. K. Hwang, A. V. Ramayya, J. H Hamilton, K. Li, C. Goodin, Y. X. Luo, J.O. Rasmussen, and S. J. Zhu, Phys. Rev. C **78**, 017303 (2008).
[29] J. K. Hwang, A. V. Ramayya, J. H Hamilton, Y. X. Luo, J.O. Rasmussen, C. J Beyer, P. M. Gore, and I. Y. Lee, *et al.*, Phys. Rev. C **67**, 014317 (2003).
[30] E. Caurier and F. Nowacki, Acta Phys. Pol. **B30**, 705 (1999).
[31] O. Perru, D. Verney, F. Ibrahim, O. Bajeat, C. Bourgeois, F. Clapier, E. Cottereau, C. Donzaud, S. Du, M. Ducourtieux, S. Essabaa, S. Gales, D. Guillemaud-Mueller, O. Hubert, C. Lau, H. Lefort, F. Le Blanc, A.C. Mueller, J. Obert, N. Pauwels, J.C. Potier, F. Pougheon, J. Proust, B. Roussiere, J. Sauvage, and O.Sorlin, Eur. Phys. J. A **28**, 307 (2006).
[32] D. Verney, private communication.